Stability and robust position control of hysteretic systems

Sina Valadkhan, Kirsten Morris, *Senior Member, IEEE*, and Amir Khajepour

Abstract

Position control of a wide class of hysteretic systems, that includes those described by a Preisach model, is considered. The main focus of this paper is stability, tracking and the trajectories of a hysteretic system controlled by a PI controller. The system output (not its derivative) is measured and controlled. It is shown that, for arbitrary reference signals, the closed-loop system is BIBO-stable with a finite gain of one. Furthermore, the absolute value of the error decreases monotonically for a constant reference signal. In this case, provided that the desired output is within the limits of the system output, zero steady-state error is guaranteed. A bound on the time required to achieve a specified error is obtained. Only a simple condition on the controller parameters is required. The results imply robust position control, even if errors in the model exist.

I. Introduction

Hysteretic systems are seen in many applications. Smart materials, such as piezoceramics, shape-memory alloys and magnetostrictive materials, are an important group of hysteretic systems. Smart actuators are generally scalable, smaller, less expensive and more efficient than traditional actuators, and hence, a competitive choice for many tasks in the industry.

Hysteresis nonlinearities are present in smart materials in varying degrees. The hysteresis can be complex and usually introduces additional memory into the system. Uncertainties seen in the physical system together with complex nonlinear behaviour of the system make it difficult to provide a robustly stabilizing controller.

Sina Valadkhan and Amir Khajepour are with the Department of Mechanical Engineering, University of Waterloo, Waterloo, Ontario, Canada, N2L 3G1 (svaladkh@uwaterloo.ca, akhajepour@uwaterloo.ca). Kirsten Morris is with the Department of Applied Mathematics, University of Waterloo, Waterloo, Ontario, Canada, N2L 3G1, (kmorris@uwaterloo.ca).

In many applications, it is desired for the smart actuator to follow a given trajectory accurately. For example in a scanning microscope where the microscope tip is driven by a smart actuator, the tip has to move to predetermined positions. Tracking errors cause distortions in the image taken. The controller has to provide stability and accurate tracking in these applications.

A popular approach for control of a hysteretic system is to linearize the system by incorporating the inverse of the hysteresis, and then design a linear controller for the resulting linear system that is close to unity [1]–[3, e.g.]. In this approach, the model must of course be invertible. Furthermore, an accurate model of the hysteretic system is required since modelling errors will affect the overall performance and could lead to instability. Even small errors in the model can lead to quite large errors in the inverse model. Also, the inclusion of the inverse of the hysteresis model in the controller leads to a complex controller. In [1], the Preisach model is coupled to an ordinary differential equation to model a magnetostrictive actuator. The model is inverted and used before the actuator to linearize the system. In [2], [3], a hysteretic system is linearized by an inverse model and $\mathbb{H}_2$ and $\mathbb{H}_\infty$ optimal control is used to provide robust stability for the linearized system.

In [4], a magnetostrictive actuator is controlled by a hybrid optimal controller. The actuator input is computed by a hysteresis model offline. A PI controller is added to compensate for unmodeled dynamics and other errors.

For a passive hysteretic system, the stability of the controlled system can be established using the passivity theorem. The passivity of the Preisach model is shown in [5] when the system output is the time-derivative of the Preisach model output. This result is used to establish L_2-stability of a velocity controller. In [6], a physics-based argument is used to prove the passivity of a magnetostrictive actuator. In this proof, no specific model is used and the results apply to any hysteresis model for magnetostrictive actuators. Passivity is used in [7] to develop an L_2-stable velocity controller for the magnetostrictive actuator.

In [8]–[11], integral control of hysteretic systems is studied using techniques for nonlinear dynamical systems. There is a common set of assumptions that the hysteretic system must satisfy, but different control system configurations are studied. In [8], pure integral control with a time-varying gain is studied, with additional dynamics included in the loop. Only constant inputs are considered. It is shown that the system is well-posed and that, if certain conditions on the time-varying gain are satisfied, the steady-state tracking error is zero. In [9], a control system

with pure integral control is studied, but this work is concerned with the asymptotic behaviour of the system in the presence of external disturbance signals in L_2. In [10], PID control of a second-order system that includes a hysteretic component (either in the forcing or the damping term) is studied. If the hysteretic component is in the forcing term and the controller parameters satisfy certain constraints that depend on the second-order system, it is shown that the system asymptotically tracks a constant input. In [11], it is shown that a time-varying controller can achieve tracking of a given signal with prescribed accuracy in a controlled system with input hysteresis. No bound on the controller gains is given. One key assumption in these results is that the system has monotonic input/output behaviour. In [12], [13] monotonicity is also used to analyse stability of systems, provided that the feedback system is well-posed in some sense. These works consider primarily systems with differential equation models. The analysis for static systems is restricted to systems where the static model is single-valued. This excludes hysteretic systems which have a characteristic looping behaviour.

The main focus of this paper is stability, tracking and the trajectories of a hysteretic system controlled by a PI controller. The system is assumed to be monotonic. The system output (not its derivative) is measured and controlled. For smart actuators, this leads to position control. We are concerned with obtaining a controller with reasonable gains that can be implemented experimentally. A PI controller was chosen because of its availability and simplicity. It is shown that, for arbitrary reference signals, the closed-loop system is bounded-input-bounded-output (BIBO) stable with a finite gain of one. Furthermore, the absolute value of the error decreases monotonically for a constant reference signal. In this case, provided that the desired output is within the limits of the system output, zero steady-state error is guaranteed. A bound on the time required to achieve a specified error is obtained. The results apply to a wide class of hysteretic systems and only a simple condition on the controller parameters is required. The results imply robust position control, even if errors in the model exist. Saturation is generally considered to be a destabilizing influence on a controlled system. However, in this approach, it is shown to assist stability.

The Preisach model [14] is one of the most important hysteresis models in the literature. While originally developed to model magnetic hysteresis, this model is frequently used for many smart materials [15]–[19]. It is shown that, in general, Preisach models satisfy the assumptions used here.

In the next section, definitions and the framework used in this paper are established. BIBO stability of the closed-loop system is shown in Section 3. Section 4 is concerned with tracking of a constant input using a PI controller. In section 5, the theory in the preceding sections is used to implement position control for a magnetostrictive actuator. The experimental results are discussed.

II. FRAMEWORK

Define $\mathbb{R}_+$ to be the set of non-negative real numbers. For any interval $I \subset \mathbb{R}_+$, let $Map(I)$ indicate the set of real-valued functions defined on I. For $T > 0$ in some interval I, the truncation of $f \in Map(I)$ to the interval $[0, T]$ is

$$f_T(t) = \begin{cases} f(t), & 0 \le t \le T, \\ 0, & T < t. \end{cases}$$

Define $\mathcal{C}(I)$ to be the set of continous functions on an interval I. The norm of a function f in $\mathcal{C}(I)$ is

$$\|f\|_\infty = \sup_{t \in I} |f(t)| .$$

Definition 1: [20] An operator $\Gamma : Map(\mathbb{R}_+) \to Map(\mathbb{R}_+)$ has the *Volterra property* if, for any $v, w \in Map(\mathbb{R}_+)$ and any non-negative T, $v_T = w_T$ implies that $(\Gamma v)_T = (\Gamma w)_T$.

Definition 2: [21] An operator $\Gamma : Map(\mathbb{R}_+) \to Map(\mathbb{R}_+)$ is *rate independent* if

$$(\Gamma v) \circ \varphi = \Gamma(v \circ \varphi)$$

for all $v \in Map(\mathbb{R}_+)$ and all continuous monotone time transformations $\varphi : \mathbb{R}_+ \to \mathbb{R}_+$ satisfying $\varphi(0) = 0$ and $\lim_{t\to\infty} \varphi(t) = \infty$.

Definition 3: [21] An operator $\Gamma : Map(\mathbb{R}_+) \to Map(\mathbb{R}_+)$ is a *hysteresis operator* if it is rate independent and has the Volterra property.

The Volterra property states that the hysteretic system output does not depend on future inputs; that is, determinism. A deterministic, rate independent operator is a hysteresis operator.

For any $\delta > 0$, $0 \le t_1 < t_2$, and any $w \in \mathcal{C}([0, t_1])$ define

$$B_1(w, t_1, t_2) := \{u \in \mathcal{C}([0, t_2]) |\ u_{t_1} = w_{t_1}\} \tag{1}$$

$$B_2(w, t_1, t_2, \delta) := \{u \in \mathcal{C}([0, t_2]) |\ u_{t_1} = w_{t_1}, \ \max_{t_1 \le \tau \le t_2} |u(\tau) - w(t_1)| < \delta\}. \tag{2}$$

Denote the hysteresis model input and output by u and y, respectively. The following assumptions are used throughout this paper.

(A1) If $u(t)$ is continuous then $y(t)$ is continuous. That is, $\Gamma : \mathcal{C}(I) \to \mathcal{C}(I)$ where I is the interval of interest.

(A2-i) (global Lipshitz property) There exists $\lambda > 0$ such that for every interval $[t_1, t_2]$ where $0 \leq t_1 < t_2$ and every $w \in \mathcal{C}([0, t_1])$, the following inequality holds for all $u_1, u_2 \in B_1(w, t_1, t_2)$.

$$\sup_{t_1 \leq \tau \leq t_2} |\Gamma(u_1)(\tau) - \Gamma(u_2)(\tau)| \leq \lambda \sup_{t_1 \leq \tau \leq t_2} |u_1(\tau) - u_2(\tau)|. \tag{3}$$

(A2-ii) (local Lipshitz property) There exists $\lambda > 0$ such that for each $t_1 \geq 0$ and $w \in \mathcal{C}([0, t_1])$, there is $\delta > 0$ and $t_2 > t_1$ such that for all $u_1, u_2 \in B_2(w, t_1, t_2, \delta)$, inequality (3) holds.

(Note by definition of $B_1(w, t_1, t_2)$ and $B_2(w, t_1, t_2, \delta)$, the Volterra property implies that $\Gamma(u_1)(\tau) = \Gamma(u_2)(\tau)$ for $0 \leq \tau \leq t_1$.)

(A3) Consider an arbitrary interval $[t_i, t_f]$. If for every $t \in [t_i, t_f]$, $u(t_i) \geq u(t)$, then $y(t_i) \geq y(t_f)$. Alternatively, if for every $t \in [t_i, t_f]$, $u(t_i) \leq u(t)$, then $y(t_i) \leq y(t_f)$.

(A4) (saturation) There exists some $u_{sat} > 0$, y_+ and y_- such that if $u(t) \geq u_{sat}$ then $(\Gamma u)(t) = y_+$ and $(\Gamma(-u))(t) = y_-$.

The global Lipshitz property (A2-i) is stronger that the local Lipshitz property (A2-ii). There is a close connection between assumption (A3) and monotonicity of the hysteretic system, in a sense that an increasing input results in increasing output and the same for decreasing inputs/outputs. By setting $t = t_f$, it is seen that if assumption (A3) holds, the hysteretic system is monotonic. The converse is not true. In Figure 1(a), a hysteretic system with a clockwise hysteresis loop is shown. This plant is monotonic, but does not satisfy assumption (A3). In Figure 1(b), a plant with a counter-clockwise hysteresis loop is shown. The plant is monotonic and assumption (A3) is satisfied.

A. Hysteretic systems represented by the Preisach model

While the results presented in this paper hold for any hysteresis model satisfying the assumptions, the Preisach model is considered here because of its general structure and applications in many hysteretic systems. In this subsection, this model is briefly explained and it is shown that the assumptions given above are satisfied. For more details about the Preisach model, see [14], [20].

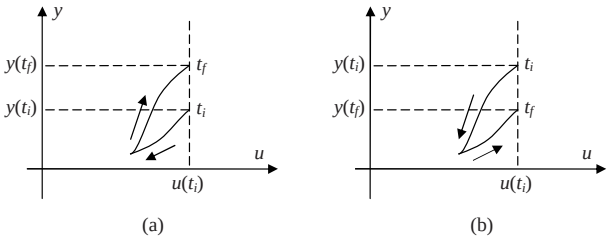

Fig. 1. (a) A clockwise hysteresis loop, and (b) a counter-clockwise hysteresis loop.

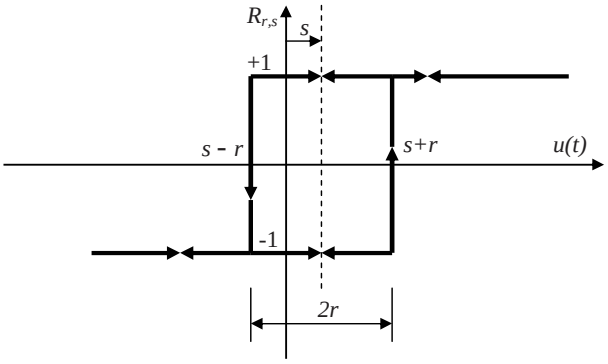

Fig. 2. The Preisach relay.

The basis of the Preisach model is the hysteresis relay shown in Figure 2. Model input, shown on the horizontal axis, is directly fed to this relay. The output of the relay, shown on the vertical axis, is used to compute the model output. Each relay is denoted by two parameters: half width r and shift s.

The output of this relay is either $+1$ or -1. The relay retains its state unless the input passes $s + r$ or $s - r$. If the relay is in the $+1$ state and the input becomes less than $s - r$, the relay switches to -1, and if the relay is in the -1 state and the input becomes greater than $s + r$, the relay switches to the $+1$ state, otherwise, the output remains the same. The relay output is only defined for a continuous input $u(t)$. As a result, the Preisach model is only valid for continuous inputs. Let $R_{r,s}[u(\cdot)](t)$ be the output of the relay with half-width r and shift s and $\mu(r, s)$ a locally integrable weight function. The output $y(t)$ of the model is

$$y(t) = \int_{-\infty}^{\infty} \int_{0}^{\infty} R_{r,s}[u(\cdot)](t)\mu(r, s)drds. \tag{4}$$

An infinite number of relays with different s and r are used. Each relay output, multiplied by a

weight function $\mu(r,s)$, contributes to form the output of the model. The weight function $\mu(r,s)$ is determined by experimental data for the hysteretic system.

The Preisach model is a hysteresis operator [20], [21]. The following theorems show that the Preisach model satisfies the assumptions under certain conditions.

Theorem 4: [20, Prop. 2.4.9,Prop. 2.4.11] If the Preisach weight function $\mu(r,s)$ satisfies

$$\lambda := 2\int_0^\infty \sup_{s\in\mathbb{R}} |\mu(r,s)|dr < \infty \tag{5}$$

then for initial Preisach boundaries in

$$\{\phi \in Map(\mathbb{R}_+) \mid |\phi(r_1) - \phi(r_2)| \leq |r_1 - r_2| \text{ for all } r_1, r_2 \geq 0\}$$

the Preisach operator maps inputs in $\mathcal{C}([t_1,t_2])$ to outputs in $\mathcal{C}([t_1,t_2])$ for any interval $[t_1,t_2]$ where $0 \leq t_1 < t_2$. For any $w \in \mathcal{C}([0,t_1])$

$$\max_{t_1\leq t\leq t_2} |y_1(t) - y_2(t)| \leq \lambda \max_{t_1\leq t\leq t_2} |u_1(t) - u_2(t)| \tag{6}$$

for all $u_1, u_2 \in B_1(w,t_1,t_2)$ where $B_1(w,t_1,t_2)$ is defined by equation (1).
The inequality (6) means that the global Lipshitz property (A2-i) is satisfied.

Many smart materials exhibit saturation [5], [15], [22]; that is, the output does not change if the absolute value of the input is larger than some limit $u_{sat} > 0$. In this case, the weight function μ has compact support; that is, $\mu(r,s) = 0$ for all $r+s$ and $r-s$ greater than u_{sat}. In all physical situations, the value of the input is constrained by actuator limitations to $|u| \leq u_{sat}$. In this situation as well, we can assume the weight function to be zero for all $r+s$ and $r-s$ greater than u_{sat}.

Theorem 5: If $\mu(r,s)$ is bounded with compact support then assumptions (A1) and (A2-i) are satisfied with the Lipshitz constant λ given by (5).

Proof: The assumptions on μ imply that (5) is satisfied. The conclusions then follows from Theorem 4. ■

For many hysteretic systems, the weight function $\mu(r,s)$ is also nonnegative [5], [15], [22].

Theorem 6: If the weight function $\mu(r,s)$ is nonnegative, assumption (A3) holds.

Proof: Assume that for every $t \in [t_i,t_f]$, $u(t_i)$ is greater than or equal to $u(t)$. Define Ω_+ to be the set of Preisach relays that are in the -1 state at t_i and the $+1$ state at t_f. Define Ω_-

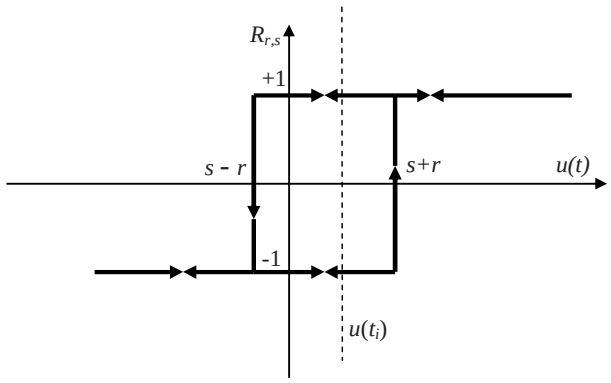

Fig. 3. Preisach relays with $s + r > u(t_i)$.

to be the set of Preisach relays that are in the $+1$ state at t_i and the -1 state at t_f. From the definition of the Preisach model,

$$y(t_f) - y(t_i) = 2 \int \int_{\Omega_+} \mu(r, s) dr ds - 2 \int \int_{\Omega_-} \mu(r, s) dr ds. \tag{7}$$

From t_i to t_f:

- For relays with $s+r > u(t_i)$: as seen in Figure 3, a transition from -1 to $+1$ cannot happen because for no t, $s + r = u(t)$. These relays cannot be in Ω_+.
- For relays with $s + r < u(t_i)$: as seen in Figure 4, at $t = t_i$, all of these relays are in $+1$ state. None of these relays can be in Ω_+.

Thus, Ω_+ is an empty set. Since $\mu(r, s) \geq 0$, the integrals in equation (7) are non-negative. Thus, as was to be shown,

$$y(t_f) - y(t_i) = -2 \int \int_{\Omega_-} \mu(r, s) dr ds \leq 0.$$

If for every $t \in [t_i, t_f]$, $u(t_i)$ is less than or equal to $u(t)$, a similar argument shows that $y(t_i)$ is less than or equal to $y(t_f)$. ■

Theorem 7: Assume that the weight function $\mu(r, s)$ is zero when $r + s$ or $r - s$ is larger than some value $u_{sat} > 0$. Define y_+ and y_- to be

$$y_+ = \int_{-\infty}^{\infty} \int_{0}^{\infty} \mu(r, s) dr ds, \tag{8}$$

$$y_- = \int_{-\infty}^{\infty} \int_{0}^{\infty} -\mu(r, s) dr ds. \tag{9}$$

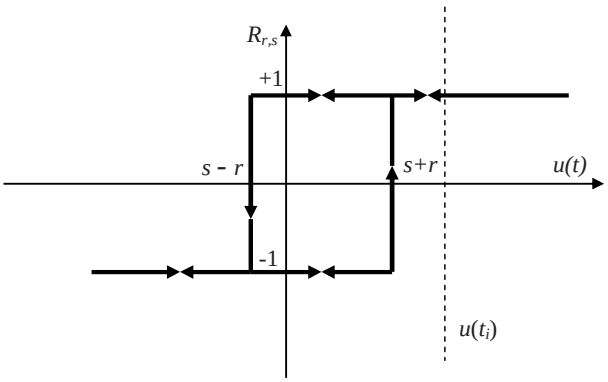

Fig. 4. Preisach relays with $s + r < u(t_i)$.

If $u(t) \geq u_{sat}$ or $u(t) \leq -u_{sat}$, the model output $y(t)$ is equal to constants y_+ or y_-, respectively; and therefore assumption (A4) holds.

Proof: Suppose that

$$u(t) \geq u_{sat}. \tag{10}$$

If the input $u(t)$ is larger than or equal to u_{sat}, all relays with non-zero weight function are in $+1$ state. (See Figure 2.) Since the relays with zero weight function do not contribute to the output, the output is y_+.

Similarly, if $u(t) \leq -u_{sat}$, the output is y_-. ■

III. Stability of the closed-loop system

In this section, the trajectories of the solutions for the closed-loop system are examined. It is shown that the system is bounded-input-bounded-output (BIBO)-stable.

Definition 8: A mapping $R : \mathcal{C}(I) \rightarrow \mathcal{C}(I)$ is BIBO-stable if for every $u \in \mathcal{C}(I)$, $Ru \in \mathcal{C}(I)$ and there exists a finite constant ρ such that

$$\|(Ru)(t)\|_\infty \leq \rho \|u\|_\infty, \ \forall u \in \mathcal{C}(I) \tag{11}$$

The smallest such constant ρ is the gain.

Consider the closed-loop feedback system shown in Figure 5, where the plant is represented by a hysteresis model Γ.

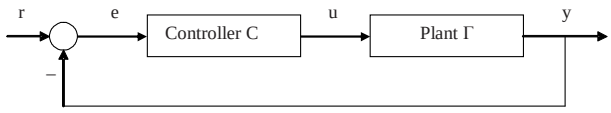

Fig. 5. The closed-loop system.

The following PI controller is used for position control:

$$\hat{C}(s) = \frac{K_I}{s} + K_P \tag{12}$$

where K_I and K_P are constants. The controller parameters are assumed only to satisfy

(B1) For the controller in (12), $0 \leq K_P\lambda < 1$ and $K_I > 0$ where $\lambda > 0$ is the Lipchitz constant in assumption (A2-i) or (A2-ii).

The following additional assumption is needed to guarantee the existence of a solution for the closed loop.

(B2) The reference signal $r(t)$ is a continuous function of time; that is, $r(t) \in \mathcal{C}(I)$ where I is the interval of interest.

The closed-loop system shown in Figure 5 is described by the following equations:

$$e(t) = r(t) - y(t), \tag{13}$$

$$f(t) = \int_0^t e(\tau)d\tau, \tag{14}$$

$$u(t) = K_P e(t) + K_I f(t), \tag{15}$$

$$y(t) = \Gamma\left[u(\cdot)\right](t). \tag{16}$$

We first show that the closed loop is well-posed; that is for continuous reference inputs $r(t)$ the above equations have a unique solution for continuous functions $u(t)$ and $y(t)$.

Theorem 9: Assume that for a hysteretic system Γ, (A3) and (A4) hold. Then $y_- \leq y(t) \leq y_+$ for every t.

Proof: Let $u(t_i)$ and $y(t_i) = (\Gamma u)(t_i)$ be the input and output respectively at some arbitrary point t_i. Suppose the input is increased monotonically from $u(t_i)$ to $u(t_f) = u_{sat}$. Assumption (A3) states that $y(t_i) \leq y(t_f)$. Since assumption (A4) states that $y(t_f) = y_+$

$$y(t_i) \leq y_+.$$

Similarly, $y(t_i) \geq y_-$. ■

We now show that the equations (13-16) have a unique continuous solution. The following existence proof uses a standard argument in differential equations.

Lemma 10: **(Existence Lemma)** Assume that (A1), (A2-ii), (B1), and (B2) hold. For any $t_0 \geq 0$ such that equations (13-16) have a unique solution for u in $[0, t_0]$, there exists $\bar{t} > 0$ such that equations (13-16) have a unique solution for $u \in \mathcal{C}([t_0, t_0 + \bar{t}))$. Furthermore, if assumption (A2-i) is satisfied,

$$\bar{t} = \frac{1 - K_P\lambda}{2\lambda K_I}. \tag{17}$$

Proof: Using (13-16), it is sufficient to show that for any $r \in \mathcal{C}([0, \infty))$

$$\begin{aligned} G(u) &= K_I \int_0^t r(\tau)d\tau + K_P r(t) \\ &\quad -K_I \int_0^t (\Gamma u)(\tau)d\tau - K_P(\Gamma u)(t) \end{aligned}$$

is a contraction on $\mathcal{C}([t_0, t_0 + \bar{t}))$ for some $\bar{t} > 0$. Assumption (A2-ii) implies the existence of a $\bar{t} > 0$ and $\delta > 0$ such that for any $w \in \mathcal{C}([0, t_0])$ and $u_1, u_2 \in B_2(w, t_0, t_0 + \bar{t}, \delta)$

$$\begin{aligned} &\max_{t_0 \leq t \leq t_0 + \bar{t}} |(Gu_1)(t) - (Gu_2)(t)| \leq \\ &(K_I\bar{t} + K_P)\,\lambda \max_{t_0 \leq t \leq t_0 + \bar{t}} |u_1(t) - u_2(t)|. \end{aligned} \tag{18}$$

Since $0 \leq K_P\lambda < 1$ and $K_I > 0$, we can obtain $(K_I\bar{t} + K_P)\lambda < 1$ by choosing $\bar{t}$ sufficiently small. It follows that G is a contraction on $\mathcal{C}([t_0, t_0 + \bar{t}))$. The Contraction Mapping Principle then implies that $u = G(u)$ has a unique solution for $u \in \mathcal{C}([t_0, t_0 + \bar{t}))$.

If assumption (A2-i) is satisfied, for every $\bar{t} > 0$, $w \in \mathcal{C}([0, t_0])$, and $u_1, u_2 \in B_1(w, t_0, t_0 + \bar{t})$, inequality (18) is satisfied. Let $\bar{t}$ be $\frac{1 - K_P\lambda}{2\lambda K_I}$. Since $0 \leq K_P\lambda < 1$ and $K_I > 0$, we have $\bar{t} > 0$ and $(K_I\bar{t} + K_P)\lambda < 1$. It follows that $u = G(u)$ has a unique solution for $u \in \mathcal{C}([t_0, t_0 + \bar{t}))$. ■

Lemma 11: Assume that (A1), (A2-ii), (B1), and (B2) hold. If u_1 is a continuous solution of (13-16) on $[0, t_1]$ and u_2 is a continuous solution on $[0, t_2]$, then $u_1(t) = u_2(t)$ for $t \leq t_o$ where $t_o = \min(t_1, t_2)$.

Proof: First, by the above lemma, there exists an interval $[0, a_o)$ on which the solution is unique. If $a_o \geq t_o$, then $u_1(t) = u_2(t)$ for $t \leq t_o$ as required. If $a_o < t_o$, then by continuity of u_1 and u_2,

$$\lim_{t \uparrow a_o} u_1(t) = \lim_{t \uparrow a_o} u_2(t).$$

Call this limit u_o. Thus, there is an unique solution to the system of equations on $[0, a_o]$. It follows from the existence lemma above that there exists δ such that there is a unique solution on $(a_o - \delta, a_o + \delta)$. Since $u_1(t) = u_2(t)$ on this larger interval, $[0, a_o]$ is not the largest interval on which the solution is unique. It follows that $u_1(t) = u_2(t)$ for $t \leq t_o$. The solution $u(t)$ does not depend on the interval of solution. ■

The following result is the main existence theorem for PI control of hysteretic systems that satisfy a local Lipshitz condition (A2-ii). Saturation assumption (A4) is used.

Theorem 12: Assume that (A1), (A2-ii), (A4), (B1), and (B2) hold. Then (13-16) have a unique solution for $u \in \mathcal{C}([0, \infty))$ and $y \in \mathcal{C}([0, \infty))$.

Proof: Let $\mathcal{T}$ be the set of all $\tau > 0$ such that there exists a solution on $[0, \tau]$. By the existence lemma, $\mathcal{T}$ is not the empty set. Define $t^* = \sup \mathcal{T}$ and $u^*[0, t^*) \to \mathbb{R}$ by

$$u^*(t) = u_\tau(t), \quad t \in [0, \tau),\ \tau < t^*.$$

Lemma 11 implies that $u^*(t)$ is well-defined and unique on $[0, t^*)$. Clearly, this is a maximal solution. The maximal interval is open. If not, and $t^* < \infty$, we could extend the solution to $[0, t^* + \delta)$ for some $\delta > 0$ using the existence lemma.

Consider now finite t^*. For $t < t^*$, since $u \in \mathcal{C}([0, t^*))$, the output $y(t) = (\Gamma u)(t)$ is also defined and assumption (A1) implies that it is in $\mathcal{C}([0, t^*))$. By Theorem 9, $|y(t)| \leq \max\{|y_+|, |y_-|\}$ for all $t < t^*$. Define

$$y^* = \lim_{t \uparrow t^*} y(t)$$

and extend $y(t)$ to $\mathcal{C}([0, t^*])$ by defining $y(t^*) = y^*$. Define

$$u^* = K_I \int_0^{t^*} r(\tau) d\tau + K_p r(t^*) - K_I \int_0^{t^*} y(\tau) d\tau - K_p y^*.$$

Then $u^* = \lim_{t \uparrow t^*} u(t)$ and we can extend $u(t)$ to $\mathcal{C}([0, t^*])$. We can then extend the solution to $[0, t^* + \delta)$ for some $\delta > 0$. This contradicts the maximality of t^*. Hence, we must have a solution $u \in \mathcal{C}([0, \infty))$. It follows that $y(t) = \Gamma u(t)$ is defined on $[0, \infty)$ and (A1) implies that $y(t)$ is in $\mathcal{C}([0, \infty))$. ■

If the hysteretic system satisfies a global Lipshitz assumption (A2-i), then saturation (A4) is not required to show existence of a unique continuous solution.

Theorem 13: Assume that (A1), (A2-i), (B1), and (B2) hold. Then (13-16) have a unique solution for $u \in \mathcal{C}([0, \infty))$ and $y \in \mathcal{C}([0, \infty))$.

Proof: Let $\mathcal{T}$ be the set of all $\tau > 0$ such that there exists a solution on $[0, \tau]$. By the existence lemma, $\mathcal{T}$ is not the empty set. Define $t^* = \sup \mathcal{T}$ and $u^*[0, t^*) \to \mathbb{R}$ by

$$u^*(t) = u_\tau(t), \quad t \in [0, \tau),\ \tau < t^*.$$

Lemma 10 states that $t^* \geq \bar{t}$, where $\bar{t}$ is defined by equation (17). Lemma 11 implies that $u^*(t)$ is well-defined and unique on $[0, t^*)$. Clearly, this is a maximal solution. The maximal interval is open. If not, and $t^* < \infty$, we could extend the solution to $[0, t^* + \delta)$ for some $\delta > 0$ using the existence lemma.

Consider now finite t^*. Since $t^* \geq \bar{t}$, we have $t^* - \frac{\bar{t}}{2} > 0$. This means that there is a unique solution in $[0, t^* - \frac{\bar{t}}{2}]$. By using Lemma 10, the solution can be extended to $[0, t^* + \frac{\bar{t}}{2})$. This contradicts the maximality of t^*. Hence, we must have a solution $u \in \mathcal{C}([0, \infty))$. It follows that $y(t) = \Gamma u(t)$ is defined on $[0, \infty)$ and (A1) implies that $y(t)$ is in $\mathcal{C}([0, \infty))$. ■

The following theorem establishes $BIBO$-stability of the closed loop. Furthermore, the system possesses unity gain for any choice of controller parameters.

Theorem 14: Assume that the closed-loop system has a unique solution for $u, y \in \mathcal{C}([0, \infty))$ and assumptions (A3), (B1), and (B2) hold. Furthermore, assume that $u(0) = 0$. If $|y(0)| \leq \|r\|_\infty$, then $\|y\|_\infty \leq \|r\|_\infty$. That is, the closed loop system is BIBO-stable with gain 1.

Proof: Define

$$L = \|r\|_\infty . \tag{19}$$

Assume that for some t_f,

$$y(t_f) > L. \tag{20}$$

Define $t_{\max u}$ to be the time at which $u(t)$ is maximized on $[0, t_f]$:

$$u(t_{\max u}) \geq u(t), \forall t \in [0, t_f]. \tag{21}$$

Define $t_{\max f}$ to be the time at which $f(t)$ defined in equation (14) is maximized on $[0, t_f]$:

$$f(t_{\max f}) \geq f(t), \forall t \in [0, t_f]. \tag{22}$$

The plant output $y(t)$ is continuous. Assumption (B2) implies that $e(t)$ is continuous. Equations (19) and (20) imply that $e(t_f) < 0$. Using continuity of $e(t)$, there is a neighborhood around t_f

on which $e(t) < 0$. Since $\dot{f}(t) = e(t)$, f is strictly decreasing in this neighborhood. As a result, $f(t)$ is not maximized at t_f:

$$t_{\max f} \neq t_f.$$

Since $e(t)$ is continuous and $\dot{f}(t) = e(t)$, $f(t)$ is continuously differentiable. If $t_{\max f} \neq 0$, maximization of $f(t)$ at $t_{\max f}$ implies that $\dot{f}(t_{\max f}) = 0$ or, $e(t_{\max f}) = 0$. Equivalently, $e(t_{\max f}) \neq 0$ implies that $t_{\max f} = 0$.

Case 1: $K_P > 0$

Using assumption (A3) and equation (21), we see that

$$y(t_{\max u}) \geq y(t_f).$$

With equation (20), this implies that

$$e(t_{\max u}) = r(t_{\max u}) - y(t_{\max u}) < 0. \tag{23}$$

By definition of $t_{\max u}$,

$$u(t_{\max u}) \geq u(t_{\max f}),$$

or from (15),

$$K_I f(t_{\max u}) + K_P e(t_{\max u}) \geq K_I f(t_{\max f}) + K_P e(t_{\max f}). \tag{24}$$

By definition of $t_{\max f}$,

$$f(t_{\max f}) \geq f(t_{\max u}). \tag{25}$$

Since K_I, $K_P > 0$, (24) and (25) imply that

$$e(t_{\max u}) \geq e(t_{\max f}). \tag{26}$$

Comparing (26) with equation (23), we obtain

$$e(t_{\max f}) < 0.$$

Since $e(t_{\max f}) \neq 0$, $t_{\max f} = 0$. From the definition of f, (14), we obtain that $f(0) = 0$. Using the definition of u, (15), we conclude that

$$u(0) = K_P e(0) < 0.$$

Thus, if $y(t_f) > L$ for some t_f, $u(0) < 0$. Similarly, if $y(t_f) < -L$, $u(0) > 0$. Thus $K_P > 0$ and $u(0) = 0$ imply that $\|y\|_\infty \leq \|r\|_\infty$.

Case 2: $K_P = 0$

Equation (15) simplifies to

$$u(t) = K_I f(t) \tag{27}$$

where $f(t)$ is defined in (14). Using (22) and (27),

$$u(t_{\max f}) \geq u(t), \forall t \in [0, t_f].$$

Since assumption (A3) holds, this implies that

$$y(t_{\max f}) \geq y(t_f). \tag{28}$$

Using (20), we conclude that

$$e(t_{\max f}) = r(t_{\max f}) - y(t_{\max f}) < 0 \tag{29}$$

and so $e(t_{\max f}) \neq 0$. It follows that $t_{\max f} = 0$. Combining equations (20) and (28), leads to

$$y(0) \geq y(t_f) > L.$$

Similarly, if $y(t_f) < -L$, $y(0) < -L$. Thus, $K_P = 0$ and $|y(0)| \leq \|r\|_\infty$ imply that $\|y\|_\infty \leq \|r\|_\infty$.

Thus, for any value of $K_P \geq 0$, $|y(0)| \leq \|r\|_\infty$ implies that $\|y\|_\infty \leq \|r\|_\infty$. The closed loop is BIBO-stable with gain 1. ■

Theorem 14 implies not only stability, but also that an overshoot, such as the one shown in Figure 6, cannot occur in the closed-loop response of the system. For hysteretic systems satisfying the saturation assumption (A4), boundedness of the output can be shown using Theorem 9. Theorem 14 extends this result to hysteretic systems that do not satisfy the saturation assumption. Also, whether or not saturation is present, the closed-loop system has a gain of 1. Even when saturation is present, the gain is determined by the above stability result, not the saturation level.

IV. TRACKING

In this section we show that PI controllers provide a closed loop system that tracks a constant input with zero steady-state error and no overshoot. A bound on the time required to achieve a specified error is obtained.

The following result guarantees that the tracking error decreases monotonically.

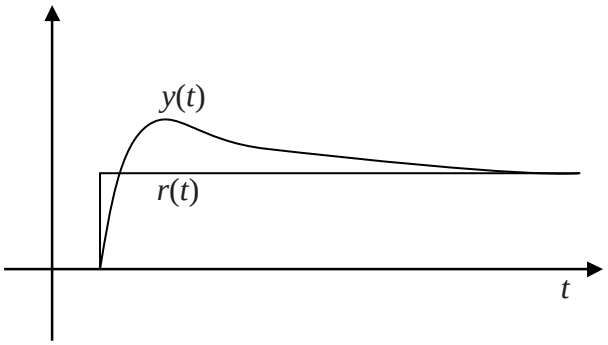

Fig. 6. An example of an overshoot.

Theorem 15: Assume that r is a constant in some interval $[t_0, T]$, the closed-loop system has a unique solution for $u, y \in \mathcal{C}([0, T])$, and assumptions (A3) and (B1) hold. If for some nonnegative ρ, $|r - y(t_0)| \leq \rho$, then $|r - y(t_1)| \leq \rho$ for all $t_0 \leq t_1 \leq T$.

Proof: Assume that for some t_1, $r - y(t_1) < -\rho$. For $r - y(t_1) > \rho$, the proof is similar.

$$e(t_1) < -\rho. \tag{30}$$

Define $t_{\max u}$ to be the time at which $u(t)$ is maximized on $[t_0, t_1]$:

$$u(t_{\max u}) \geq u(t), \forall t \in [t_0, t_1]. \tag{31}$$

Define $t_{\max f}$ to be the time at which $f(t)$ is maximized on $[t_0, t_1]$:

$$f(t_{\max f}) \geq f(t), \forall t \in [t_0, t_1].$$

Since the plant output $y(t)$ is continuous, $f(t)$ is continuously differentiable. Inequality (30) implies that $\dot{f}(t_1) = e(t_1) < 0$, and so $f(t)$ is strictly decreasing in the vicinity of t_1. This implies that

$$t_{\max f} \neq t_1.$$

If $t_{\max f} \neq t_0$, maximization of $f(t)$ at $t_{\max f}$ implies that $\dot{f}(t_{\max f}) = 0$, or,

$$e(t_{\max f}) = 0, \text{ if } t_{\max f} \neq t_0. \tag{32}$$

By definition of $t_{\max f}$ and $t_{\max u}$,

$$u(t_{\max f}) \leq u(t_{\max u}), \tag{33}$$

$$f(t_{\max f}) \geq f(t_{\max u}). \tag{34}$$

Using (15) and (33)

$$K_P e(t_{\max f}) + K_I f(t_{\max f}) \leq K_P e(t_{\max u}) + K_I f(t_{\max u}).$$

But inequality (34) implies that

$$K_P e(t_{\max f}) \leq K_P e(t_{\max u}). \tag{35}$$

Using assumption (A3) and (31) we obtain that

$$y(t_{\max u}) \geq y(t_1),$$

and so,

$$e(t_{\max u}) \leq e(t_1). \tag{36}$$

Case 1: $K_P > 0$

By combining (30), (35), and (36) we have

$$e(t_{\max f}) < -\rho \leq 0. \tag{37}$$

Since $e(t_{\max f}) \neq 0$, (32) implies that $t_{\max f} = t_0$. Rewriting inequality (37) leads to

$$e(t_0) = r - y(t_0) < -\rho$$

as required.

Case 2: $K_P = 0$

Equation (15) simplifies to

$$u(t) = K_I f(t).$$

Since $K_I > 0$, any choice for $t_{\max u}$ is also a choice for $t_{\max f}$. At $t_{\max f}$, $u(t)$ is maximized. By repeating the argument above for (36) we obtain that

$$e(t_{\max f}) \leq e(t_1).$$

Using inequality (30) leads to

$$e(t_{\max f}) < -\rho \leq 0.$$

Similar to the previous case, $e(t_{\max f}) \neq 0$ and (32) imply that $t_{\max f} = t_0$ and so

$$e(t_0) = r - y(t_0) < -\rho.$$

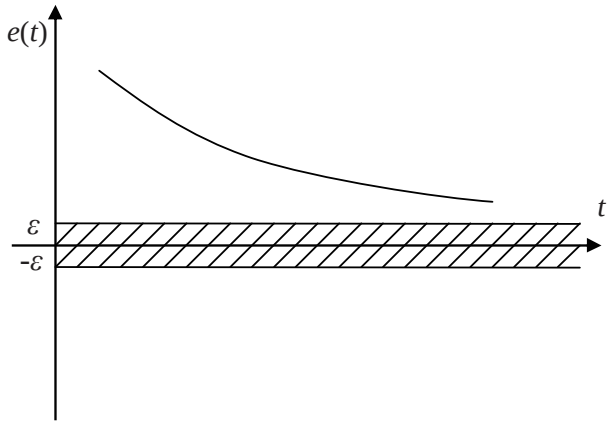

Fig. 7. The error $e(t)$ versus time.

The proof is complete. ■

Theorem 15 states that during a period where the input is constant, the absolute value of the error is never increased. As a result, an oscillatory response or an overshoot cannot be seen. The following theorem proves that, if in addition to the assumptions of the previous theorem, the saturation assumption (A4) holds, then the error can be made arbitrarily small.

Theorem 16: Let t_0 be a non-negative real number. Assume that $r(t)$ is a constant, r, in $[t_0, \infty)$, the closed-loop system has a unique solution for $u, y \in \mathcal{C}([0, \infty))$, and that assumptions (A3), (A4), and (B1) hold. If $y_- \leq r \leq y_+$, then for every $\varepsilon > 0$,

$$|r - y(t)| \leq \varepsilon, \forall t \geq \bar{t} + t_0,$$

where

$$\bar{t} = \frac{\frac{u_{sat}}{K_I} + |f(t_0)|}{\varepsilon}. \tag{38}$$

Consequently, $\lim_{t\to\infty} y(t) = r$.

Proof: Assume that for some ε and $t \geq \bar{t} + t_0$, $r - y(t) > \varepsilon$. The proof for the case $y(t) - r > \varepsilon$ is identical.

Theorem 15 implies that for all $t' \in [t_0, t]$,

$$|r - y(t')| = |e(t')| > \varepsilon. \tag{39}$$

This is illustrated in Figure 7.

Integrating from t_0 to $t_0 + \bar{t}$, we have

$$\int_{t_0}^{t_0+\bar{t}} e(t')dt' \geq \varepsilon\bar{t}.$$

Using the definition of f, (14), it follows that

$$f(t_0 + \bar{t}) \geq f(t_0) + \varepsilon\bar{t}. \tag{40}$$

Since $\bar{t}$ is defined by (38),

$$\varepsilon\bar{t} \geq \frac{u_{sat}}{K_I} - f(t_0). \tag{41}$$

Substituting this into (40) leads to

$$f(t_0 + \bar{t}) \geq \frac{u_{sat}}{K_I}.$$

Since $t \geq \bar{t} + t_0$, (39) implies that

$$e(t_0 + \bar{t}) > \varepsilon. \tag{42}$$

By using equation (15), a bound on $u(t_0 + \bar{t})$ can be obtained:

$$u(t_0 + \bar{t}) \geq K_P\varepsilon + u_{sat} \geq u_{sat}.$$

Using assumption (A4), $y(t_0 + \bar{t}) = y_+$. From (42),

$$r > y_+.$$

Thus, if $r - y(t) > \varepsilon$ for some $t \geq \bar{t} + t_0$, $r > y_+$. Similarly, if $y(t) - r > \varepsilon$, then $r < y_-$. Hence, $y_- \leq r \leq y_+$ implies that $|r - y(t)| \leq \varepsilon$ for all $t \geq \bar{t} + t_0$ as was to be shown.

It was shown that for every $\varepsilon > 0$, there is a $\bar{t}$ such that $|r - y(t)| \leq \varepsilon$ for all $t \geq \bar{t} + t_0$. This is the definition of limit. Thus, $\lim_{t\to\infty} y(t) = r$. ■

Theorem 16 gives an upper limit for the time required to achieve any accuracy ε. Theorem 9 shows that an output smaller than y_- or larger than y_+ is not feasible. The condition $y_- \leq r \leq y_+$ is just that the desired reference point is within these saturation limits. The above theorem states that if the input to the closed loop is within the saturation limits, zero steady-state error is guaranteed.

Theorem 14 can be used to design a controller for position control. The controller must only satisfy assumptions $0 \leq \lambda K_P < 1$ and $K_I > 0$. In the next section, a position controller is designed and evaluated experimentally.

V. EXPERIMENTAL RESULTS

In the previous sections, tracking and stability for position control of hysteretic systems were shown for a PI controller. In this section, these results are used to develop a stabilizing position controller for a magnetostrictive actuator.

To evaluate the position controller experimentally, a magnetostrictive actuator is used. In this actuator, a rod made of Terfenol-D, a magnetostrictive material, provides actuation. This material reacts to a magnetic field. In the presence of a magnetic field, this material generates a small mechanical displacement. The displacement is measured by an optical encoder with a resolution of $10nm$.

To provide the requested magnetic field, the Terfenol-D rod is used inside an electrical magnet. The magnet is powered by a programmable electrical current source. The current source is controlled by a PC computer. Several sensors are included in the actuator to measure flux density and temperature. The sensors' measurements are sent to the PC computer. MATLAB Real-Time Workshop® is used with the PC computer. The controller is implemented within MATLAB.

Terfenol-D cannot withstand tension and should be in compression for proper operation. The compression is provided by a set of washer springs. The springs are soft enough that it can be assumed that the compression force is constant when the Terfenol-D rod changes size. The force of the springs can be adjusted. The force is measured by a load cell.

For a magnetostrictive material, magnetic field H and magnetization M are the input and output, respectively. The relation between magnetic field H and magnetization M can be represented by a Preisach model with a positive weight function with compact support [15]. Assumptions (A1)-(A4) are satisfied.

In most applications, it is desired to control the displacement λ produced by the actuator. The following equation relates magnetization M to displacement [15], [23]:

$$\lambda = \gamma_1 M^2 + \gamma_2 M^4 \tag{43}$$

where γ_1 and γ_2 are constants at a constant mechanical load. Using this relation, position control is achieved by controlling the magnetization M.

To find the magnetization in the magnetostrictive actuator, the displacement produced is measured and equation (43) is used to compute magnetization. The same relation is used to

compute the desired magnetization and hence, errors in (43) do not affect the closed-loop performance.

Theorem 14 states that any PI controller satisfying assumption (B1) provides stability. To find the optimal gains for the controller, a performance criteria is needed. Here, tracking performance is used; that is, an optimal set of controller parameters should minimize the cost function

$$J = \int_{t_1}^{t_2} (y - r)^2 dt,$$

where r is the reference input, y is the closed-loop output and $[t_1, t_2]$ is the time range of interest, subject to the parameter constraints (B1). A smaller value of J means a closer match between the actual and desired outputs.

Because of the nonlinear and complex structure of the system, the only method for minimizing J is numerical optimization. For this purpose, the closed-loop is simulated by using a Preisach model with a general weight function. The model is identified in [15]. Using the Preisach model, y is computed as a function of controller parameters. The cost function J is numerically minimized using Nelder-Mead simplex direct search method [24] with a reference signal r chosen as a series of step inputs. Formally, the ideal version of such a reference input is not continuous. However, in experiment there is a rapid but continuous change between values and so the signal is continuous. (Furthermore, due to the nature of a hysteresis operator, there is no difference between the output of a hysteretic system with a step discontinuity and one with a smooth monotonic change between the same values [20].)

The optimum values for the controller gains are: $K_I = 38.02 s^{-1}$ and $K_P = 0.0785$. The optimal gains were tested experimentally for different reference signals.

In Figure 8, the closed-loop response of the system to step input is shown for the optimized controller. Excellent tracking is seen. As predicted by Theorem 16, there is no steady-state error. In Figures 9 and 10, portions of the response are magnified. The nonlinear nature of the system exhibits different responses in different conditions. The system settles to $\pm 10nm$ of the reference signal in $0.175s$ and $0.122s$ in Figures 9 and 10, respectively. This is within the accuracy of the sensor used. A small overshoot is seen in Figures 9 and 10. In Figure 9, some oscillations are also observed. Theorem 15 implies that there is no oscillatory response or overshoot. The overshoots and oscillations are likely caused by some unmodeled mass in the system. Simulation results are also shown in Figures 9 and 10. Since unmodeled dynamics are not present in the

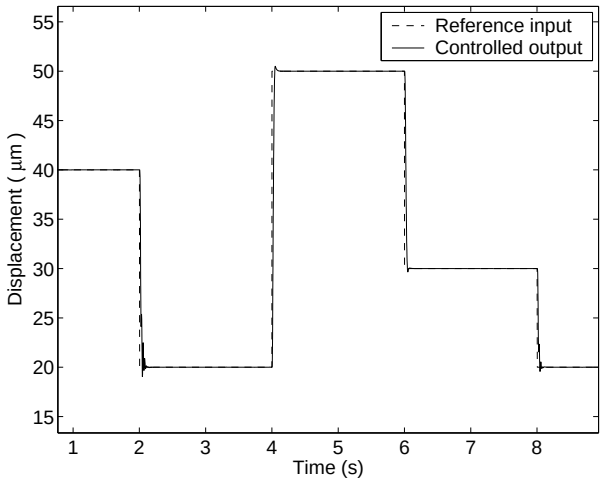

Fig. 8. The closed-loop response to various steps.

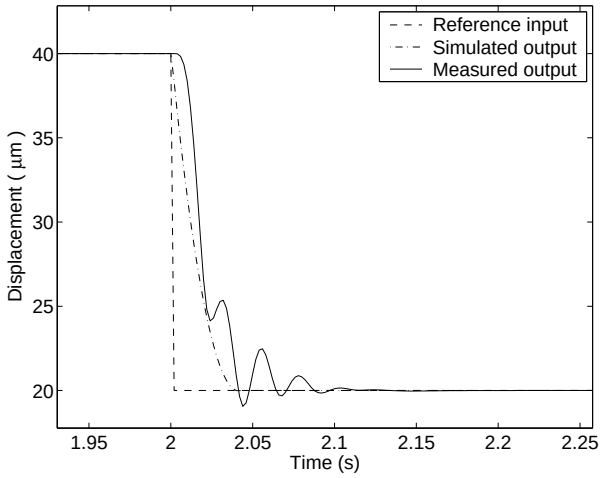

Fig. 9. Transient response after a step. The effects of a moving mass are seen.

simulation, no overshoot or vibrations are seen. This is consistent with the results of Theorem 15.

In Figure 11, the system response to a sinusoidal input with varying amplitude is displayed. In the previous sections, it was shown that the closed-loop system is BIBO-stable for variable reference signals. Stability is observed and the reference trajectory is followed accurately. In Figure 12, the tracking error for the same experiment is shown. The root-mean-square tracking

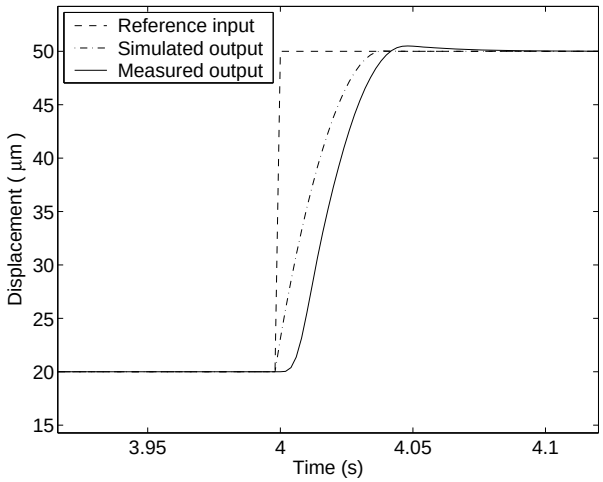

Fig. 10. Transient response after a step. No vibration is seen.

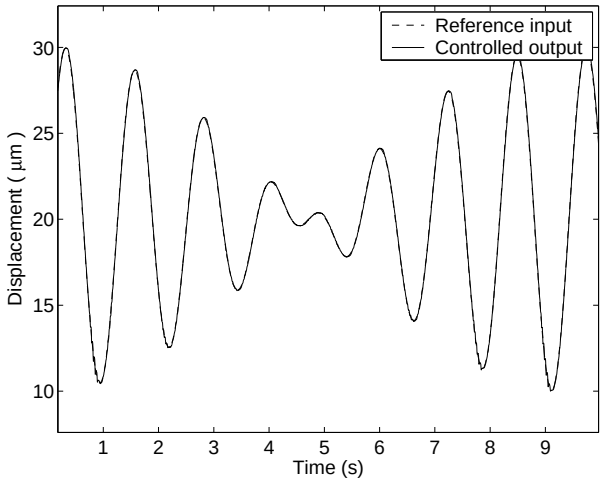

Fig. 11. Tracking response of the closed loop.

error is $0.11\mu m$, a relative error of 1.1%.

REFERENCES

[1] X. Tan and J. S. Baras, "Modeling and control of hysteresis in magnetostrictive actuators," *Automatica*, vol. 40, no. 9, September 2004, pp. 1469-1480.

[2] J. M. Nealis and R. C. Smith, "Model-based robust control design for magnetostrictive transducers operating in hysteretic and nonlinear regimes," *IEEE transactions on control systems technology*, vol. 15, no. 1, January 2007, pp. 22-39.

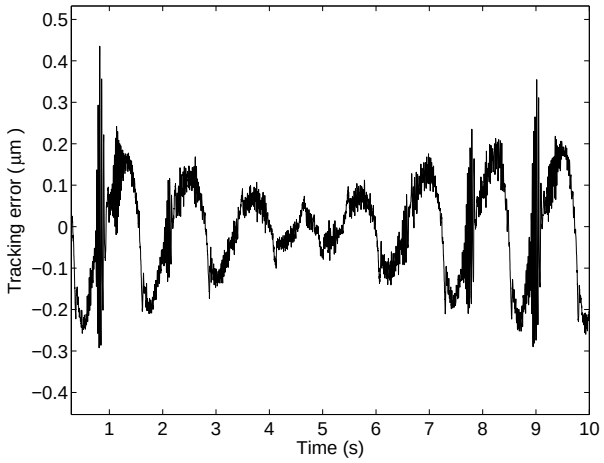

Fig. 12. Tracking error of the closed loop.

[3] ——, "Robust control of a magnetostrictive actuator," *Proceedings of SPIE, the international society for optical engineering*, vol. 5049, 2003, pp. 221-232.

[4] W. S. Oates and R. C. Smith, "Nonlinear perturbation control for magnetic transducers," *Proceedings of the 45th IEEE conference on decision and control*, 2006, pp. 2441-6.

[5] R. B. Gorbet, K. A. Morris, and D. W. L. Wang, "Passivity-based stability and control of hysteresis in smart actuators," *IEEE transactions on control systems technology*, vol. 9, no. 1, January 2001, pp. 5-16.

[6] S. Valadkhan, K. A. Morris, and A. Khajepour, "Passivity of magnetostrictive materials," *SIAM Journal of applied mathematics*, vol. 67, No. 3, 2007, pp. 667-686.

[7] ——, "Robust control of smart material-based actuators," *New Frontiers in Control Theory and Applications*, edited by V. Blondel, S. Boyd, and H. Kimura, Springer-Verlag, 2008.

[8] H. Logemann, E. P. Ryan, and I. Shvartsman, "Integral control of infinite-dimensional systems in the presence of hysteresis: an input-output approach," *ESAIM - control, optimisation and calculus of variations*, to appear.

[9] ——, "A class of differential-delay systems with hysteresis: asymptotic behaviour of solutions," *Nonlinear analysis*, submitted.

[10] B. Jayawardhana, H. Logemann, and E. P. Ryan, "PID control of second-order systems with hysteresis," *preprint*.

[11] A. Ilchmann, H. Logemann, and E. P. Ryan, "Tracking with prescribed transient performance for hysteretic systems," *preprint*.

[12] D. Angeli and E. Sontag, "Monotone control systems," *IEEE Trans. on Automatic Control*, vol. 48, no. 10, Oct. 2003, pp. 1684-99.

[13] ——, "Multi-stability in monotone input/output systems," *Systems and Control Letters*, vol. 51, no. 3-4, 2004, pp. 185-202.

[14] I. Mayergoyz, *Mathematical models of hysteresis and their applications*. Amsterdam, Boston: Elsevier Academic Press, 2003.

[15] S. Valadkhan, K. A. Morris, and A. Khajepour, "A review and comparison of hysteresis models for magnetostrictive materials," *Journal of intelligent material systems and structures*, submitted.

[16] R. B. Gorbet, D. W. L. Wang, and K. A. Morris, "Preisach model identification of a two-wire SMA actuator," *Proceedings, IEEE international conference on robotics and automation*, vol. 3, 1998, pp. 2161-7.

[17] D. Hughes and J. T. Wen, "Preisach modeling of piezoceramic and shape memory alloy hysteresis," *Smart materials and structures*, vol. 6, 1997, pp. 287-300.

[18] S. B. Choi and Y. M. Han, "Hysteretic behavior of a magnetorheological fluid: experimental identification," *Acta mechanica*, vol. 180, No. 1-4, 2005, pp. 37-47.

[19] X. Zhou, J. Zhao, G. Song, and J. D. Abreu-Garcia, "Preisach modeling of hysteresis and tracking control of a Thunder actuator system," *Proceedings of SPIE - the international society for optical engineering*, vol. 5049, 2003, pp. 112-125.

[20] M. Brokate and J. Sprekels, *Hysteresis and phase transitions*. New York: Springer, 1996.

[21] M. Brokate, "Hysteresis operators," *in Phase transitions and hysteresis*, edited by A. Visintin, Springer-Verlag, Berlin, 1994, pp. 1-38.

[22] R. C. Smith, M. J. Dapino, and S. Seelecke, "Free energy model for hysteresis in magnetostrictive transducers," *Journal of applied physics*, vol. 93, no. 1, 1 January 2003, pp. 458-466.

[23] D. C. Jiles, "Theory of the magnetomechanical effect," *Journal of physics D: applied physics*, vol. 28, no. 8, 14 August 1995, pp. 1537-1546.

[24] D. P. Bertsekas, *Nonlinear Programming*. Belmont, Massachusetts: Athena Scientific, 1999.